2025 IMEKO TC26 International Conference on
Metrology for Archaeology and Cultural Heritage
Bergamo, Italy, October 15-17, 2025

Biofilms on limestones specimens: laboratory tests implementing a non-destructive approach

Davide Ripamonti[1†], Emanuele Frabasile[5], Alessia Marzanni[2], Chao Gao[3], Chiara Bertolin[3], Villa Federica[4] and Nicola Gherardo Ludwig[1]

[1]*Department of Physics "A. Pontremoli", Università degli Studi di Milano, via Celoria 16, 20133 Milano, Italy, davide.ripamonti@unimi.it, nicola.ludwig@unimi.it*
[2]*Faculty of Agricultural, Environmental and Food Sciences, Libera Università di Bolzano, Piazza Universitá 5, 39100 Bolzano, Italy; alessia.marzanni@student.unibz.it*
[3]*Department of Mechanical and Industrial engineering, Norwegian University of Science and Technology, Richard Birkelands vei 2B, Trondheim, 7491, Norway; chiara.bertolin@ntnu.no, chao.gao@ntnu.no*
[4]*Department of Food, Environmental and Nutritional Sciences, Università degli Studi di Milano, Via Celoria 2, 20133 Milano, Italy; federica.villa@unimi.it*
[5]*Department of Environmental Sciences and Policies, Università Degli Studi di Milano, Via Celoria 2, 20133 Milano, Italy; emanuele.frabasile@studenti.unimi.it*

Abstract **– This study explores the potential protective role of subaerial biofilms (SABs) in conserving stone heritage, challenging the traditional view of microbial colonization as merely damaging. SABs, composed of microorganisms embedded in extracellular polymeric substances (EPS), may form a stabilizing barrier that reduces stone surface porosity and water permeability. The research examines the long-term effect of SABs on water dynamic under moisture stress conditions (30% RH, 25 °C). We assessed water absorption, evaporation, and visual surface changes using non-invasive techniques. Findings contribute to a growing body of evidence suggesting that SABs, under specific conditions, can serve as eco-compatible alternatives to synthetic coating to preserve cultural heritage.**

I. INTRODUCTION

In recent years, cultural heritage conservation has increasingly turned to sustainable, even nature-based solutions to mitigate the progressive degradation of historic materials. Stone monuments represent enduring symbols of human history and culture, yet their preservation is increasingly compromised by environmental factors [1,2]: continuous exposure to atmospheric agents—such as rain, wind, and solar radiation—can significantly weathering the structural and aesthetic integrity of stone surfaces, making them more vulnerable to fractures and erosion [3,4]. Historically linked to biodeterioration and visual damage, microbial biofilms are now being reconsidered for their potential protective roles [5,6]. Subaerial biofilms (SABs) are structured microbial consortia that develop on exposed lithic substrates, adapting to both the mineral composition of the stone and the surrounding atmosphere [7]. These complex microbial ecosystems are encased in a self-produced matrix of extracellular polymeric substances (EPS) - primarily polysaccharides and proteins – which can form a stabilizing layer between the stone and the environment, potentially mitigating weathering processes [8,9]. Recent studies have demonstrated that, under certain conditions, biofilms reduce surface porosity and water permeability, thereby acting as a natural barrier rather than a harmful agent [10,11].

This contribution investigates the long-term effect of different SABs on water dynamic under moisture stress conditions (30% of relative humidity at 25 °C). Non-destructive methods (i.e., reflectance spectrophotometry, capillary water absorption, and evaporation flux) are used to assess water absorption and evaporation dynamics, as well as the long-term visual effects on the stone surface.

II. MATERIALS AND METHODS

A. SABs' cultures and types of stones

SABs examined in this study were categorized as mono- and dual-species based on their composition. Mono-specie biofilms consisted solely of the photosynthetic cyanobacterium *Synechocystis* sp. PCC 6803, while dual-species biofilms included both *Synechocystis* sp. and the chemoorganotrophic bacterium *Escherichia coli* K12 MG1655. Axenic cultures of the photosynthetic

cyanobacterium *Synechocystis* sp. PCC 6803 and the chemoorganotrophic bacterium *Escherichia coli* K12 MG1655 were grown separately in Blue-Green (BG11) and Luria-Bertani (LB) media, respectively. Once cultures reached the stationary phase, cells were collected by centrifugation, rinsed with BG11 medium, and resuspended to a final density of approximately 10^8 cells/ml. For dual-species inoculation, equal volumes of *Synechocystis* and *E. coli* suspensions were mixed, while mono-species *Synechocystis* cultures were adjusted to a concentration of ~5 × 10^7 cells/ml, following the procedure described by Villa et al. (2015) [12]. Both mono-species (*Synechocystis* only) and dual-species (*Synechocystis* + *E. coli*) SABs were developed in a modified Drip Flow Reactor (DFR), as outlined in the growth protocol described in [12].

Table 1. Characteristics of the studied specimens at the start of testing in 2025.

Samples	Weight [g]	Area [cm^2]	SABs` type	Sample exposure
B1	33.17	14.6	-	under 30% RH since 2023
B2	29.50	14.3	-	under 30% RH since 2023
P1	34.89	15.7	Dual	under 30% RH since 2021
P2	31.04	14.9	Dual	under 30% RH since 2021
C1	32.78	14.2	Mono	under 30% RH since 2023
C2	30.02	15.1	Mono	under 30% RH since 2023
D5	30.48	14.6	Dual	under 30% RH since 2023
D6	31.66	15.4	Dual	under 30% RH since 2023
N	39.09	18.7	Dual	under 30% RH since 2024

Samples used in this investigation (B1, B2; P1, P2; C1, C2; D5, D6 and N) are listed in Table 1. Mono and dual-species SABs were grown on identical limestone specimens, each measuring approximately 75 mm × 23 mm × 10 mm, similar in size to a microscope glass slide. The limestone composition is about 90% calcite and dolomite and 8.91% of porosity (Table 1 and Fig. 1).

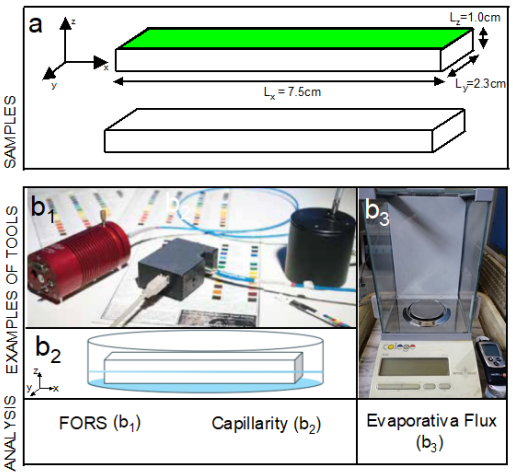

Fig. 1. (a) Geometry of a biofilm coverage and control sample (B ones); (b) tools carried on for investigation and characterization, (b1) FORS - Fiber optics reflectance spectroscopy [13], (b2) capillary set-up; (b3) evaporative flux measurements.

B. Laboratory environment and techniques

SAB-colonized (P1, P2; C1, C2; D5, D6) and control (uncolonized, B1 and B2) limestone samples were placed, after DFR, in individual desiccator chambers and kept at a constant temperature of 25°C and 30% relative humidity (RH), monitored with digital thermo-hygrometers Tzone Digital Technology Co., Ltd until 2025 (see Table 1) to simulate a stressed-aging situation. The N sample, instead, was kept under non-controlled conditions (a natural room environment, i.e., T= 21°C and RH= 45%) until 2024; then, the sample was kept under the 30% RH for about one year (2024-2025). To obtain representative data, each test was repeated on three different areas of the specimen's surface. Capillary Water Absorption and the Evaporation Flux were used to evaluate changes in the physical properties of the stones with and without SABs, while the reflected light - Fiber Optics Reflectance Spectroscopy – was applied to study the alterations in stone appearance.

FORS - Reflectance Spectrophotometry

Reflectance spectrophotometry analyses the apparent behavior of an illuminated object based on its emission spectrum; the light beam from the source is directed through a fiber optic cable [13]. Depending on the wavelength, the emitted radiation allows for qualitative analysis, providing insight into the material's characteristics and enabling its identification. The system is centered around a primary light source—specifically, a halogen lamp (HL 2000, 12.24 Volt)—and is configured with a bifurcated fiber optic cable that channels light first toward the surface of the sample and then, as reflected radiation (acting as a secondary source), back to the electromagnetic signal processor

(Ocean Optics HR4000), which is connected to a computer. The signal, once converted into electrical form, is displayed graphically as reflectance R, via the corresponding software of the signal processor.

Capillary Water Absorption

The capillary absorption test evaluates the water uptake behavior of porous solid materials upon temporary contact with a liquid, providing insights into both surface characteristics and internal pore structure [14]. Porosity, defined by the network of fine interconnected pores, governs the movement of fluids within the material. In this test, a 9 cm shallow dish is filled with demineralized water to a depth of approximately 5 mm. Test specimens are sealed on all sides with parafilm, leaving only the biofilm surface of interest exposed, to ensure unidirectional water absorption. Each sample is partially immersed (5 mm) with the exposed face oriented downward, allowing the capillary rise to act against gravity. After immersion, specimens are briefly placed on absorbent paper to remove excess surface water without disturbing absorbed moisture. Gravimetric measurements were carried out using a Mettler Toledo College balance with a maximum capacity of 150 g and a resolution of 0.1 mg. The balance was connected to a computer for automated data collection and placed on a vibration-damped, perfectly horizontal surface, inside a glass chamber with sliding doors for adequate air circulation. Samples were tested sequentially, with non-tested specimens stored in a sealed container to reduce evaporative loss. Immersion intervals (repeated ten times) start at 10 seconds, then increase to 30 seconds, after that 1-minute intervals, to monitor during both rapid and slower absorption phases. The methodology is based on the UNI EN 15801:2010 standard for capillary water absorption, with modifications to immersion times, measurement intervals, and specimen dimensions tailored to the study's requirements.

Evaporation flux

Another method used to characterize the water-related properties of the stone involved prolonged immersion to achieve full saturation of the sample under analysis, followed by the recording of mass loss during the subsequent evaporation phase. This approach allows for a quantitative analysis of the water initially retained by the solid matrix and the water vapor released through desorption via the evaporative flux, or evaporation rate (ER), that quantifies the exchange of water between the liquid and vapor phases [15]. Then, the variation in mass over a defined time interval was monitored, beginning with a fully water-saturated stone specimen. In this case the water content (WC) was one of the key parameters to measure i.e., the difference in mass between the wet and dry states over the dry mass; then the flux (Ω), computed as the change in mass (Δm) divided by the time interval (Δt) and the surface area (S) of the sample. For the evaporation phase, a 2-liter capacity cylinder was used to ensure full saturation of the specimen, with sufficient pressure to facilitate complete water absorption. Distilled water was used to avoid any mineral alteration of the rock's composition during the immersion. To prevent bacterial contamination, the water was replaced after each immersion. The immersion period was set to a minimum of two days, ensuring complete sample saturation. After removal from the water, each specimen was wrapped in parafilm, leaving only the test surface exposed—similar to the procedure used in the capillary absorption test, but with the goal of restricting evaporation solely to the exposed surface. Gravimetric measures to capture evaporation dynamics were carried out using the Mettler Toledo College balance with an automated data acquisition system to record the mass at 10-minute intervals.

III. RESULTS

Fiber optics reflectance spectroscopy

The graphical representation in Fig.2 displays the reflected light portion R expressed as a percentage of the wavelength. Due to the sensitivity of the instruments, the data are included along the electromagnetic spectrum, ranging from near ultraviolet (380 nm) to near infrared (900 nm), encompassing the visible range (380-780 nm). From the characteristic white tint and opacity of the limestone in most of the samples, high levels of reflectance are established, which remain stable at around 70% of the incident light (Fig. 2). A slight deviation from this is observed in C1, which shows slightly lower and more irregular levels in the reflectivity spectrum, particularly between 400 and 650nm.

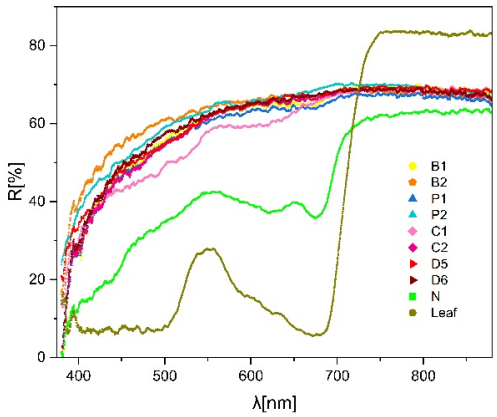

Fig. 2. Reflectance of the samples along the electromagnetic spectrum between 380 and 900 nm.

Distinctly, the N (light green in Fig.2) shows that in the

visible spectrum up to 700 nm, no light reflection levels exceed 40%. Starting from shorter wavelengths, the increasing portion of reflected light remains around 40% in the green (550 nm), then decreases to approximately 30% in the visible red, with the exception of a peak at 650 nm. For even greater wavelengths, the levels of both surfaces increase rapidly and stabilize beyond 750 nm, a trend observed in all other samples. When comparing the spectra of the N sample with that of a typical green leaf (Fig. 2, dark green) within the green wavelength range, a notable similarity is observed, suggesting the presence of photosynthetic green pigments on the stone (Fig. 2); this is probably due to the non-controlled conditions kept in the initial part of the investigation.

Capillary Absorption

The absorption dynamics are most evident in the early phase of the test, when the sample has a greater capacity to retain water. For this reason, in Fig. 3, measurements of water absorption Φ (in terms of mass on surface, y-axis) are plotted as a function of the square root of time (x-axis).

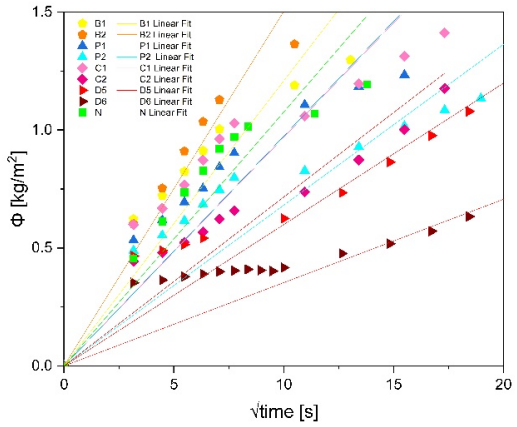

Fig. 3. Sample surface water absorption trends Φ over time. Solid lines represent linear fit trendlines.

Additionally, each data series ends at the mass value corresponding to 99% saturation for the specimen. In Fig. 3, the data can therefore be approximated using a linear fit regression, where the slope defines the capillary absorption coefficient (C). To enable comparison across stones of different sizes, each coefficient was normalized with respect to the exposed surface area. From Fig.3, the control stones exhibit the highest absorption capacities, with coefficients C of 0.121 kg/(m^2√s) (B1) and 0.150 (B2). Among the specimens coated with extracellular polymeric matrix, decreasing coefficients C are observed from the monoculture samples (C1 – 0.096, and C2 – 0.072) to the dual-species cultures P2, D5 and D6—respectively showing the lowest value (0.068, 0.060 and 0.035), corresponding to a total absorption time approximately twice that of its counterpart. An exception is sample P1, with a coefficient of 0.097, which falls between the two specimens colonized by mono-species SABs. As for specimen N (0.108), although the heterogeneous substrate type maintains some absorptive capacity relative to similar samples, it does not reach the absorption levels of the original stone material.

Evaporative Flux

Due to the rock's specific porosity, the sample's mass loss during evaporation follows a characteristic L-shaped curve [15]: a rapid vapor release in the first ten hours, followed by a gradual decline, stabilizing around 24 hours, indicating near-dry conditions. To compare evaporation trends (Ω) across samples with varying dimensions and measurement intervals, water content (WC) was analyzed. Results show a relatively steady and elevated evaporation rate in the early phase, driven by the evaporation of surface-adhered water. Only after this thin film is evaporated, the internal moisture starts to diffuse outward. These patterns may also reflect instrumental variability or fluctuations in humidity and temperature in the laboratory.

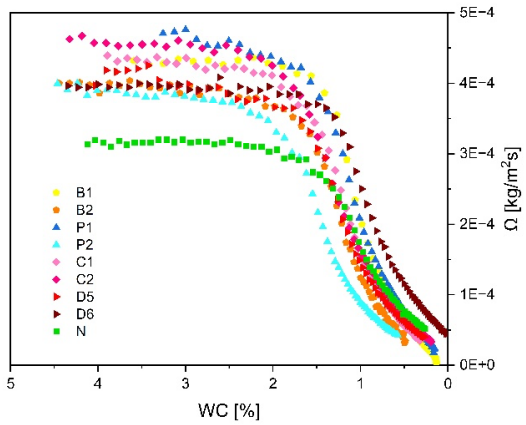

Fig. 4. Vapor flux over time across the sample surface, expressed in kg/m²·s. Data points are plotted as a function of water content WC within the stone. Flux values were recorded at regular intervals of 10 minutes, except for sample B1 (15-minute intervals).

Thus, the analysis focuses on the first 12 hours of evaporation, with the average maximum flux calculated from the stable portion of this period, excluding the initial surface-water phase from the maximum flux values (Fig. 4). The control stones (B) show average levels compared to the other specimens. Specimens (C1) and (C2) exhibit higher evaporation rates, while (D5) and (D6) —showing lower values—are comparable to the B samples. Specimen (P1), one of the oldest ones, displays the most intense flux, probably due to the

highest decay, likely influencing its evaporation behavior. Specimens P2 and N exhibited the lowest flux values. However, the surface of N shows flux levels like the other samples. Notably, the initial values for this last specimen were significantly lower, possibly due to greater water adhesion to the surface, which then evaporated rapidly.

IV. DISCUSSION AND CONCLUSION

This study simulated microclimate aging conditions in the laboratory to investigate the effects of SABs on stone properties, including capillary absorption, wettability, and evaporative water flux. Specimens were grouped based on type of SABs and exposure history, with samples from the same lithic material showing varying behaviors. Under prolonged exposure to dry conditions, samples colonized by dual-species SAB- (groups P and D) exhibited lower capillary absorption, suggesting pore obstruction by the biofilm components, in contrast to the mono-species SAB samples C, which showed the opposite results. Evaporation tests revealed that colonized stone samples exhibited water release rates similar to or higher than untreated control samples, with group C displaying particularly high flux. The N specimen, with visible green organic residues, also showed surface-dependent differences, particularly with a high capillarity absorption coefficient and a low evaporation flux, as displayed with FORS.

Overall, the water-based tests indicate differences between uncolonized stones and those covered by SABs, suggesting that mature SABs and their residues influence the stone's hydric properties. Dual-species SABs notably impact stone moisture dynamics, displaying the lowest C coefficient and evaporative flux, and they tend to accumulate water. The N sample shows, unlike the dual P and D samples, a high C, probably due to the property of the SAB to retain water, reducing evaporation. The mono-species samples, on the other hand, exhibit behavior very similar to that of the control samples, indicating that the drying state has decreased the water-retaining capacity SAB.

These findings highlight the complex interactions between SABs and the lithic substrates underneath, highlighting biofilm's contribution to stone weathering and preservation. While this study focused on physical properties, future research integrating microbiology will help clarify the broader implications of biofilm effects on stone preservation, as an eco-compatible, in a well-known circular economy context, alternative to artificial coating to preserve cultural heritage, also in term of visible patinas.

REFERENCES

[1] Gorbushina, A. Life on the rocks. Environmental Microbiology, 9(7), 1462-2912, 2007.

[2] Gaylarde, C., Little, B. Biodeterioration of stone and metal - Fundamental microbial cycling processes with spatial and temporal scale differences, Science of The Total Environment, 823, 153193, 2022.

[3] Gorbushina, A. Life on the rocks. Environmental Microbiology, 9(7), 1462-2912, 2007.

[4] Quansheng L., Chengyu L., Dong H., Changyu W. Comparative Study on the Deterioration of Surface Physical and Mechanical Properties of Sandstone Cultural Heritage Under Different Dissolution Conditions. Applied Sciences. 15. 4310, 2025.

[5] Gadd, G. M., Dyer, T.D. Bioprotection of the built environment and cultural heritage. Microbial Biotechnology, 10(5), 1152-1156, 2007.

[6] Villa, F., Stewart, P. S., Klapper, I., Jacob, J. M., Cappitelli, F., Subaerial Biofilms on Outdoor Stone Monuments: Changing the Perspective Toward an Ecological Framework. BioScience, 285–294, 66(4), 2016.

[7] Villa, F., Cappitelli, F. The Ecology of Subaerial Biofilms in Dry and Inhospitable Terrestrial Environments. Microorganisms, 7(10), 380 (2019).

[8] Vázquez, N. D., Silva, B., Prieto, B. Influence of the properties of granitic rocks on their bioreceptivity to subaerial phototrophic biofilms, Science of The Total Environment, 610-611, 44-54, 2018.

[9] Villa, F., Ludwig, N., Mazzini, S., Scaglioni, L., Fuchs, A.L., Tripet, B., Copié, V., Stewart, P.S., Cappitelli, F. A desiccated dual-species subaerial biofilm reprograms its metabolism and affects water dynamics in limestone. Science of The Total Environment 868, 161666, 2023

[10] Yong-Hui L., Ji-Dong G. A more accurate definition of water characteristics in stone materials for an improved understanding and effective protection of cultural heritage from biodeterioration. International Biodeterioration & Biodegradation, 166, 2022.

[11] Melada, J.; Villa, F.; Giudici, M.; Battaglia, I.; Carangelo, E.; Marzanni, A.; Ripamonti, D.; Ludwig, N. Investigating the Role of Subaerial Biofilms in Cultural Heritage Conservation with Infrared Thermography. Eng.Proc., 51, 18, 2023.

[12] Villa, F., Pitts, B., Lauchnor, E., Cappitelli, F., & Stewart, P. S. Development of a laboratory model of a phototroph-heterotroph mixed-species biofilm at the stone/air interface. Frontiers in Microbiology, 2015.

[13] Cosentino A. FORS, Fiber Optics Reflectance Spectroscopy con gli spettrometri miniaturizzati per l'identificazione dei pigmenti. Archeomatica. 1. 16-22, 2014.

[14] Feng C. and Janssen H.. Hygric properties of porous building materials (III): Impact factors and

data processing methods of the capillary absorption test. Building and Environment, 2018

[15] Le Bray Y., Prat M. Three-dimensional pore network simulation of drying in capillary porous media. International Journal of Heat and Mass Transfer, volume 42, Issue 22, pages 4207-4224, 1999.